Journal of the European Ceramic Society **15** (1995) 33–43
© 1995 Elsevier Science Limited
Printed in Great Britain. All rights reserved
0955-2219/95/$9.50

Processing, Microstructure and Mechanical Properties of SiC Platelet-reinforced 3Y-TZP Composites

A. Selçuk, C. Leach & R. D. Rawlings

Department of Materials, Imperial College of Science, Technology and Medicine, London, SW7 2BP, UK

(Received 25 March 1994; revised version received 1 June 1994; accepted 30 June 1994)

Abstract

A study has been carried out on the processing of silicon carbide platelet-reinforced yttria-stabilised zirconia ceramics, using slip casting techniques followed by cold isostatic pressing and pressureless sintering. Optimisation of the process variables, in particular the stability and homogeneity of the composite slurry and mould configuration, enabled samples with good platelet alignment and densities >96% of theoretical to be produced routinely after pressureless sintering. The pore formation and desintering phenomena in the presence of platelets are explained in relation to the microscopy and dilatometry results. The decreases in the room-temperature fracture toughness and flexural strength with increasing platelet content are attributed to the reduction in transformation hardening and the increase in porosity.

1 Introduction

Recent studies on SiC whisker-reinforced yttria-stabilised tetragonal zirconia ceramics (Y-TZP) have shown considerable improvements in fracture toughness since the stress-induced martensitic transformation toughening in the matrix is coupled with whisker toughening, which is achieved by the combination of mechanisms, including crack pinning,[1] crack deflection,[2] crack bridging, and pull-out.[3–5] The fracture toughness of SiC whisker–3Y-TZP composite can be increased up to about 12 MPa $m^{1/2}$ at the expense of a decrease in strength to about 670 MPa.[6] Whisker reinforcement leads to improvements in strength at high temperatures where the positive modulus load transfer reduces the effective stress at the crack tip.[6] The high-temperature toughness of the composite is expected to be governed by whisker toughening mechanisms, since transformation toughening becomes less effective with increased temperature, and does not operate above a critical temperature (≈700°C for Y-TZP).

Whiskers, however, due to their geometry, are a severe health hazard when inhaled.[7] Furthermore, the formation of a whisker network in the ceramic matrix introduces constraints on the sintering, leading to a considerable reduction of sintered density.[8–10] The densification to closed porosity in these composites often requires the application of pressure and a much higher sintering temperature than that for the monolithic material. One way to overcome these problems is the use of silicon carbide platelets (SiC_p), which are thought to offer similar mechanical property improvements to those of whisker-reinforced TZPs with minimal associated health hazard and at a reduced cost. The comparable effects of SiC platelets to whiskers in improving toughness have been demonstrated in SiC platelet-reinforced alumina[11] and mullite.[12]

For SiC platelets distributed randomly in a ceramic matrix at a concentration over 10 vol.%, the geometrical arrangement of platelets has been found to inhibit densification to full density under pressureless sintering conditions.[13] Hence the overall strength is expected to be reduced by the platelets, which act as Griffith flaws. When the platelets are oriented parallel to the tensile stress axis, the defect size is effectively reduced to the thickness of the platelets and the constraints on sintering are eased, due to a better sinter shrinkage being achieved in the matrix material between the parallel planes of platelets. Thus, the reduction of strength with platelet content can be minimised by the optimisation of composite processing conditions to yield denser materials through control of the platelet orientation.

The study reported here is concerned with the slip casting, cold isostatic pressing and sintering of

SiC_p–3mol%Y-TZP composites and the resultant mechanical properties microstructural characteristics, such as preferred orientation of platelets, porosity and grain boundary and SiC/matrix interface structure. The change in strength and fracture toughness with the platelet content is related to the observed microstructural features.

2 Experimental

2.1 Materials and processing

The matrix material used for the production of SiC_p–3Y-TZP composites in this study was the commercially available tetragonal zirconia powder with 3 mol% Y_2O_3 content (TZ-3YS, Tosoh Corporation, Japan), designed for slip casting operations. TZ-3Y powder of the same composition and particle size as those of TZ-3YS powder, but with a smaller primary crystallite size (25 nm) and a larger specific surface area (15·4 m^2/g), was used for the preliminary tests on slurry preparation and slip casting operations. The properties of both powders are listed in Table 1. The silicon carbide platelets (SiC_p) were of 99·9% pure stoichiometric α-phase (Third Millennium Technologies Inc., USA, -400 mesh grade) with 10 μm average diameter and 0·5–3 μm thickness.

Figure 1 shows the processing route used for the preparation of the green structures of 3Y-TZP containing 10 and 20 vol.% SiC_p. Prior to processing in the composite, the SiC platelets were subjected to acid (0·2M HNO_3 solution) and base (0·1 5M NH_4OH solution) washes for 24 h in order to remove leachable impurities and to enhance the dispensability of platelets in water. Each wash was followed by the repeated dispersion of platelets in deionised water and filtering until the suspensions reached a constant pH. The platelets were then rinsed in ethanol, which was found to minimise agglomeration on drying and the subsequent processes in aqueous solution.

Stable composite slurries of SiC_p and 3Y-TZP powder were prepared by mixing the constituents in proportion in deionised water at pH 3 using a

Table 1. Properties of TZ-3Y and TZ-3YS powders

	TZ-3Y	*TZ-3YS*
Composition, wt%		
Y_2O_3	5·13	5·06
Al_2O_3	<0·005	<0·005
SiO_2	<0·002	<0·002
Fe_2O_3	0·004	0·002
Na_2O	0·022	0·005
Particle size, μm	0·3	0·3
Crystallite size, nm	25·1	36
Specific surface area, m^2/g	15·4	6·3

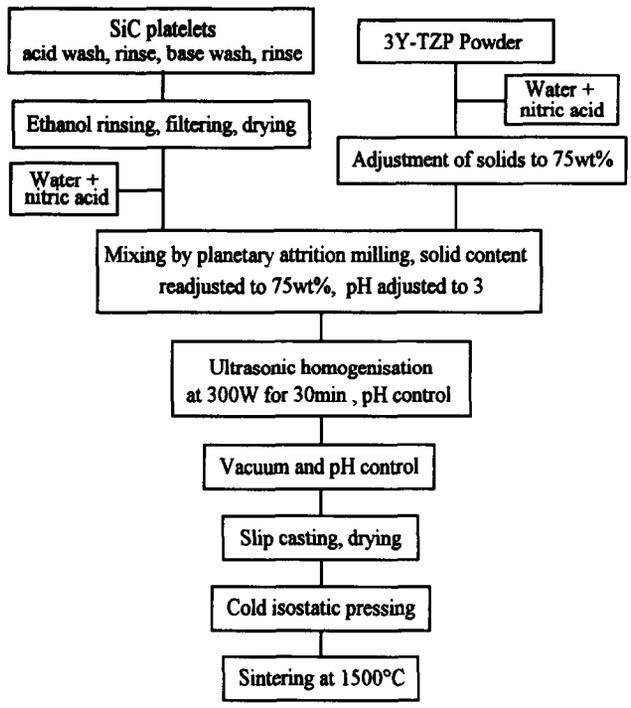

Fig. 1. Processing chart of SiC platelet–3Y-TZP ceramic composites.

planetary attrition mill with an agate container and ball. The pH was adjusted during mixing by the addition of dilute HNO_3 solution. The solid loading of the resultant slurries was always maintained at 75 wt%. Subsequent tests showed that the slurries were stable at pH 3 after planetary milling for 30 min, suggesting that sufficiently high electrostatic repulsive forces were generated to avoid flocculation. The agglomerates that were present in the as-received 3Y-TZP powder could not be broken up by the planetary milling. Ultrasonic dispersion was employed at 300W for 30 min for complete deagglomeration and homogeneous dispersion of the slurries after planetary milling. The entrapped gas in the slurry was removed under vacuum. pH 3 was maintained throughout above procedures. The final composite slurries showed very good stability and slip-casting properties.

For slip casting, samples with 0, 10 and 20 vol.% SiC platelet contents were formed into bars (48 mm × 12 mm × 10 mm) such that the SiC platelets, which orientate parallel to the mould surfaces during casting, would be parallel to the tensile stress axis of the four-point bend tests employed in the present work. Sample geometry and plaster mould configuration are shown schematically in Fig. 2. The slip-cast bars were dried at 40°C for 24 h, followed by heating at 120°C for 4 h and cold isostatic pressing at a pressure of 175 MPa. The green density was determined from the measured weight and volume of samples. Sintering behaviour of samples was

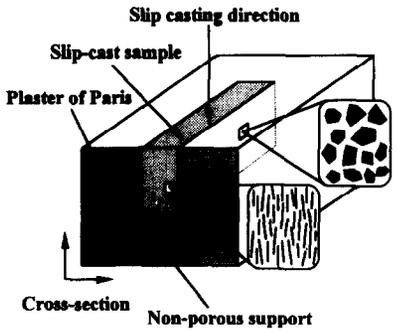

Fig. 2. Schematic configuration of a plaster mould and a sample on slip casting.

characterised by dilatometry on heating up to 1500°C at a heating rate of 4°C/min. Samples prepared for microstructural examination and mechanical testing were sintered at 1500°C for 3 h in flowing Ar atmosphere in a high-temperature graphite resistance furnace lined with impervious alumina tube to permit the control of supplied atmosphere. Heating and cooling rates of 3°C/min and 4°C/min respectively, were employed for the sintering of all samples. The sintered density and the percentage open porosity was measured by the Archimedes water-displacement technique.[14]

2.2 Specimen preparation and mechanical testing

Test pieces, containing 0, 10 and 20 vol.% SiC platelets sintered to >96% of theoretical density, were ground to produce flexural bend test specimens (38 mm × 3 mm × 3 mm) and single-edge notch beam specimens, SENB, (38 mm × 6 mm × 3 mm where $W = 2B = 6$mm) using diamond grinding wheels at 60 mm/s. For both types of specimens, the prospective tensile surfaces were kept parallel to the plane at which the platelets were aligned during slip casting so that the crack propagation direction was always perpendicular to the plane of the platelet alignment. The tensile surfaces of all flexure bars were polished through to 1 μm diamond lapping and the edges were bevelled. A straight notch, having a root radius of 80–100 μm, was introduced to each SENB specimen using a 0·15 mm thick SiC slitting disc of a sharp end profile. The relative notch depth (a/W) was in the range 0·1 to 0·12.

A four-point bend test fixture, with an inner span of 15 mm and an outer span of 20 mm, and a servo hydraulic testing machine were employed for the evaluation of fracture strength and toughness. The displacement during tests was monitored by the use of two transducers, situated at the mid-span and the outer span of each specimen. Thus, any displacement associated with the test rig was eliminated from the actual displacement of the specimen by recording the differential output from the transducers using a signal conditioning unit. At least five specimens were tested for each composition at a cross-head speed of 0·5 mm/min to determine the room-temperature strength and toughness. From the results of four-point bend tests, flexural strength, σ_b, was calculated using the equation:

$$\sigma_b = \frac{3}{BW^2}\frac{P(s-L)}{2} \tag{1}$$

where P is the applied load, s the inner span, L the outer span, B the specimen breadth and W the specimen width. The fracture toughness, K_{IC}, was determined by:

$$K_{IC} = \frac{6}{BW^2}\frac{P(s-L)}{4}Ya^{1/2} \tag{2}$$

where the geometric factor, Y, is given by:[15]

$$Y = 1{\cdot}99 - 2{\cdot}47(a/W) + 12{\cdot}97(a/W)^2 - 23{\cdot}17(a/W)^3 + 24{\cdot}8(a/W)^4 \tag{3}$$

2.3 Microstructural investigations

Phase identification after sintering was performed by X-ray diffraction using CuK_α radiation. The extent of the phase transformation from tetragonal to monoclinic structure in the matrix phase, induced by fracture toughness testing, was determined from the integrated X-ray intensity of diffraction lines, $I_{m,t}(hkl)$, of the monoclinic and tetragonal phases, using the following equations:[16]

$$X_m = \frac{I_m(111) + I_m(11\bar{1})}{I_m(111) + I_m(11\bar{1}) + I_t(111)} \tag{4}$$

where X_m is the integrated intensity ratio for monoclinic phase, which yields the volume fraction

$$V_m = \frac{PX_m}{1 + (P-1)X_m} \tag{5}$$

where $P = 1{\cdot}311$ for tetragonal–monoclinic mixtures.

The microstructures of sintered bars and the features on fracture surfaces after mechanical tests were characterised by scanning electron microscopy (SEM). The orientation distribution of platelets at different sections of slip-cast and sintered samples was determined using an optical image analysis system. For each section, at least five SEM pictures, corresponding to over 2000 platelets, were analysed.

3 Results and Discussion

3.1 Consolidation of SiC_p-reinforced zirconia structures

Slip casting followed by cold isostatic pressing is a suitable method for the production of composites where a uniform distribution and preferred orien-

tation of reinforcing agents, such as platelets, are required. High green densities, no damage to the platelets during processing, and the ease and inexpensive production of composite components are the additional advantages of the slip-casting process. However, the production of electrostatically stabilised homogeneous composite slips for the best slip casting properties depends on the simultaneous adjustment of a number of variables.

The casting characteristics are influenced primarily by the morphology, surface quality and dimensional characteristics of the starting powders. Other parameters, such as pH value, viscosity, homogeneity and solid concentration, are of particular importance to maintain the maximum colloidal stability of slurries. A commonly employed means of obtaining a well-dispersed suspension is to impart a repulsive surface charge on particles by pH adjustment. In the present case, the optimisation of the slurry variables is complicated by the presence of SiC platelets that are of different composition, size, geometry and surface quality from the matrix material. Uniform distribution and electrostatic stabilisation of both phases in the composite slurry were achieved by the acid/base surface treatment of SiC platelets, planetary mixing of the constituents in aqueous media, adjustment of solid loading, and high power ultrasonic dispersion, in sequence, accompanied by continuous pH adjustment (Fig. 1).

As observed for SiC whisker-reinforced ceramic composites,[8] the suspension stability of SiC platelets was the major factor in determining a pH that would provide codispersion of zirconia particles and platelets in dense slurries. The zeta potential, measured on dilute suspensions of platelets over a pH range of 2 to 9, showed that the moderate to high levels of surface charge necessary for the electrostatic stabilisation of the slurry occur at pH $\leq$ 3. This is in agreement with the previous electrophoresis mobility and viscosity measurements of SiC whisker suspensions.[17,18] It was further reported that the modification of whisker surface chemistry, by either surface oxidation or acid and base washing of whiskers, enhances the electrostatic stabilisation of the suspensions. Since the presence of free SiO_2 at the oxidised surfaces of SiC platelets is not desired for the zirconia matrix, the acid/base washing technique was adopted in the present processing.

Concerning the zirconia matrix phase, the recent work of Nikumbh *et al.*[19] on slip casting slurries of TZ-3YS powder has shown that the slips with $\leq$75 wt% solid content at pH $\leq$ 4 gives minimum viscosity with Newtonian flow behaviour in which the electrostatic repulsive forces at particles are large and the viscosity remains constant with the change in shear rate. They also observed that the viscosity of the slurry increases drastically when the solid loading (solid/liquid ratio) exceeds 75 wt% ($\approx$35 vol.%) ZrO_2. In the present work, the preliminary slip-casting tests on slurries of TZ-3Y and TZ-3YS powders, each containing 20 vol.% SiC platelets, revealed that stable slurries of low viscosity and with good flow behaviour can be formed at pH 3 providing solid loadings of $\leq$50 wt% for TZ-3Y powder and $\leq$75 wt% for TZ-3YS powder are used. The chemical composition and the particle size of both powders were the same and the higher solid content achieved in the slurries of TZ-3YS powder was attributed to its lower specific surface area and a higher crystallite size than those for TZ-3Y powder (Table 1). Also, slip casting times for SiC_p-TZ-3Y composite slurries to form 10 mm thick samples were as short as 1 h compared to 3 h required when TZ-3Y powder was used. Therefore, all samples for mechanical tests were prepared using TZ-3YS powder.

Although the mechanical mixing and the adjustment of pH and solid content were successful in forming stable slurries, there were always soft agglomerates of particles and platelets, inherited from the original materials. Complete deagglomeration of composite slurries were achieved using an ultrasonic probe at 300W output power for 30 min. The agitation caused by ultrasonic waves also served to increase the homogeneity of the slurry. Other workers have found similar results for the ultrasonic dispersion of SiC whisker–Al_2O_3 composites without the use of deflocculants.[8,20]

The achievement of a high green density and a strong preferred orientation of platelets was the main advantage of slip casting over other processing techniques. As shown in Fig. 3, the slip casting bar samples without SiC platelets yielded a relative green density of 55%, but this increased to 60% with increasing platelet content. The increase in green density is due to substitution of the

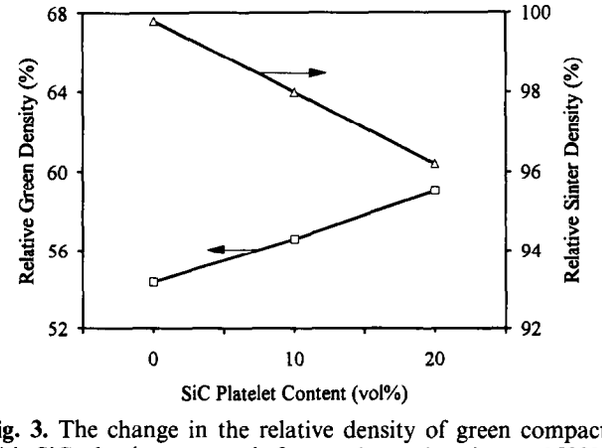

Fig. 3. The change in the relative density of green compacts with SiC platelet content before and are sintering at 1500°C for 3 h.

matrix and its porosity by fully dense SiC platelets. A further increase of the green density by around 2% was achieved by cold isostatic pressing.

3.2 Sintering characteristics

The plots of relative linear shrinkage, dL/L_o, and linear shrinkage rate, $d(dL/L_o)/dT$, as a function of temperature for a slip-cast 3Y-TZP sample and a composite containing 20 vol.% SiC_p are shown in Figs 4 (a) and (b), respectively. The dependency of the sinter shrinkage on platelet orientation was not studied in the present work and the plots for the composite sample in Fig. 4 are for data obtained in a direction perpendicular to the plane in which the basal plane of platelets are preferentially oriented. It follows that dL/L_o at a given temperature is the relative shrinkage of the matrix regions between the basal planes of platelets.

As shown in Fig. 4 (a), the shrinkage of both samples starts at around 900°C and the sintering curves are identical up to 1200°C, at which point the platelets starts inhibiting the sintering of the composite. The shrinkage of the composite up to 1200°C is referred to as the first stage sintering. This is followed by a period of negligible shrinkage until the second stage sintering commences at around 1250°C. The two stages of sintering are revealed by the presence of two successive peaks on the sintering rate plot for the composite (Fig. 4(b)) as the sintering rate approaches zero at the plateau region of the shrinkage plot and then starts increasing at ≈1250°C reaching a maximum at ≈1400°C. In contrast, the sintering rate plot for the monolithic material shows a single peak with a maximum at ≈1400°C.

Under isothermal conditions, the sintering temperature was chosen as 1500°C in order to enhance the density of the matrix, particularly in the presence of platelets. Sintering at 1500°C for 3 h yielded relative densities that depended on the SiC_p content but were >96% (Fig. 3). The relative densities obtained in the present study were superior to those of similar composites produced by other processing techniques, e.g. 91% and 94% for 20 vol.% Al_2O_3 platelet-reinforced 12Ce-TZP and 3Y-TZP composites, respectively, each pressureless sintered at 1500°C.[21] X-Ray diffraction analysis of sintered samples revealed only the presence of SiC phase and tetragonal zirconia with no detectable monoclinic phase.

As shown in Fig. 3, the sintered density reduced while the green density increased with SiC_p content. Near theoretical density (6070 kg/m^3) was easily achieved on sintering the monolithic material. However, densification in the platelet-reinforced zirconia systems depended on the flow and sintering of the matrix between platelets. An increase in platelet content resulted in partial inter-platelet bridging that hindered particle rearrangement in the matrix and thus lead to the formation of elongated crack-like pores at the platelets, as exemplified by the micrograph in Fig. 5. The number of pores increased in the regions where the platelets were

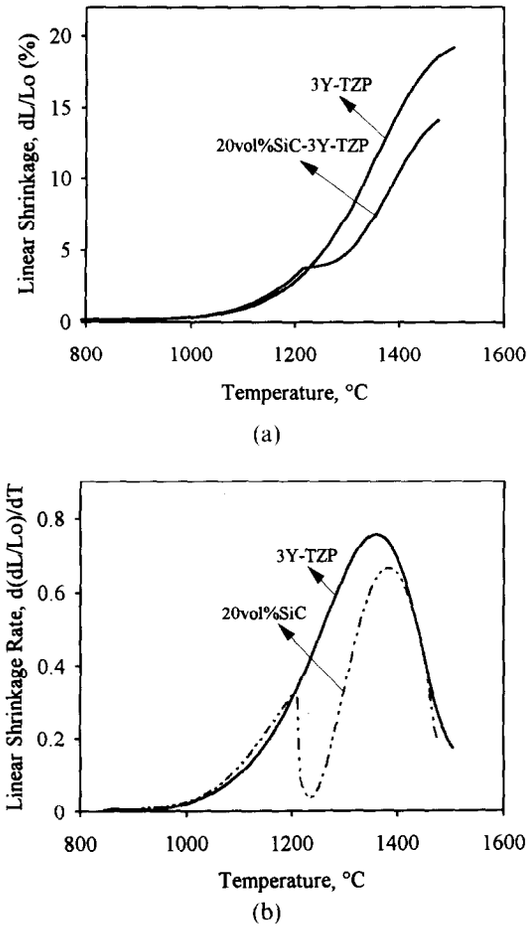

Fig. 4. (a) The relative linear shrinkage and (b) the linear shrinkage rate of 3Y-TZP and 20 vol.% SiC_p reinforced 3Y-TZP compacts on non-isothermal sintering at a heating rate of 4°C/min.

Fig. 5. An SEM micrograph from the cross-section of a 20 vol.% SiC platelet reinforced 3Y-TZP composite, revealing crack-like voids and porosity associated with platelets as shown by arrows.

bridged or the density of platelets was relatively high. The crack-like pores are unlikely to be reduced by increasing the sintering temperature but could probably be closed by applying pressure during sintering.

Previous work on the effect of inclusions on densification[22–24] has already demonstrated that the underlying phenomenon for the interruption of sintering in the presence of rigid particles is the development of localised strains in the porous matrix. The type and magnitude of the matrix strains change with the location in the matrix, inter-platelet distance and the geometrical arrangement, volume fraction and size of platelets in the surrounding volume.[23,24] Therefore the densification of the matrix is heterogeneous. A region under localised compressive stress densifies first, producing non-deformable networks where the porosity tends towards zero.[22,23] These highly dense regions are expected to constrain the shrinkage of the adjacent porous matrix by inducing hydrostatic tensile stresses, which finally leads to desintering and the formation of local porosity. Hence the overall sintering rate is reduced with increasing ratio of the hydrostatic tensile stress to the compressive sintering stress of the matrix, σ_h/Σ_m.[25,26]

In view of these observations, it is considered that the two-stage sintering process in the 20 vol.% SiC_p–3Y-TZP composite can be explained in terms of the development of compressive and tensile stresses in the matrix. That is, the first stage of sintering in the composite sample (Fig. 4) is attributed to the free sintering of the matrix until heterogeneous densification and the compressive and tensile stresses develop in the matrix. This is evident from the sinter shrinkage plots for the monolithic and the composite samples being identical at temperatures up to 1200°C. The following reduction in the sintering rate is related to a rapid densification at locations between closely spaced SiC platelets while relatively high porosity is retained in the remaining matrix.

The onset of the increase in shrinkage at the second stage of sintering may be explained by the thermal activation at temperatures >1250°C being large enough for the growth of highly dense networks at the expense of the pore growth in the adjacent porous matrix. The porous regions under the hydrostatic tensile stresses go through desintering and the formation of crack-like voids at the SiC platelet–matrix interface. This can occur provided the hydrostatic tensile stresses are large enough to induce the break up of grain bridges linking polycrystalline clusters in porous regions.

To summarise, high sintered densities were achieved in these composites by slip casting and pressureless sintering, although the formation of some voids on sintering was unavoidable. It may be that the pressureless-sintered density can be further increased to a level, possibly close to theoretical density, by the use of SiC platelets with relatively small thickness, provided that slip-cast-

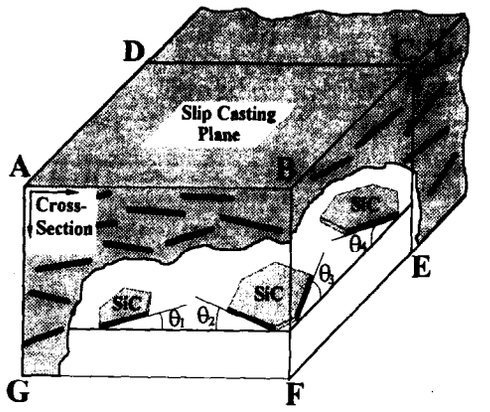

Fig. 6. Schematic of three dimensional array of platelets in a slip-cast sample, showing the edge lines of platelets observed in the ABFG and BCEF planes, in tilted positions at angles, θ_i with the slip casting plane (ABCD). The BCEF plane is perpendicular to the mould face (ABCD) and the ABFG plane is the cross-section of a bar sample.

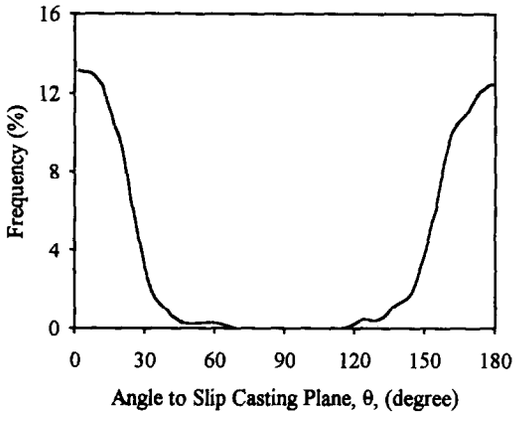

(a)

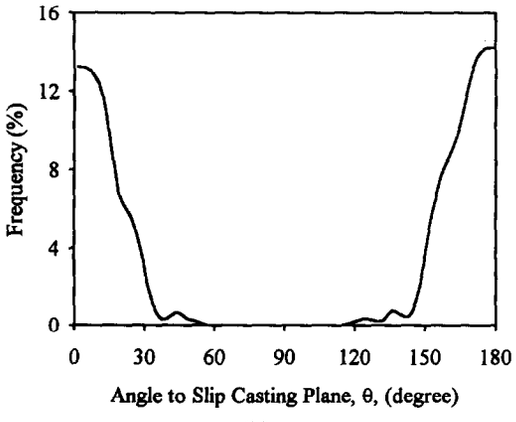

(b)

Fig. 7. The orientation distribution of SiC platelets in relation to the slip-casting plane (the mould surface) observed in the ABFG planes of bar samples (Fig. 6), containing (a) 10 vol.% and (b) 20 vol.% SiC platelets.

ing results in a very strong preferred orientation of platelets.

3.3 Orientation distribution of platelets after sintering

The effect of slip casting on the orientation distributions of SiC platelets was studied by determining the frequency of platelets (%), oriented with their basal planes at a given angle, θ, to the porous mould face (ABCD in Fig. 6) which is referred to as the slip-casting plane. Figures 7(a) and (b) show the plots of platelet frequency as a function of θ, taken from the sections (BCEF in Fig. 6) perpendicular to the slip-casting plane, for composite samples containing 10 and 20 vol.% SiC_p, respectively. Both plots show that θ for the majority of platelets is within $\Delta\theta = \pm 30°$. The corresponding SEM micrographs, shown in Figs 8(a) and (b), exemplify the platelet distribution and orientation presented in the frequency–angle plots; it is clear from these micrographs that there is a strong preferred orientation with the basal platelet planes, mostly in close alignment with the slip-casting plane.

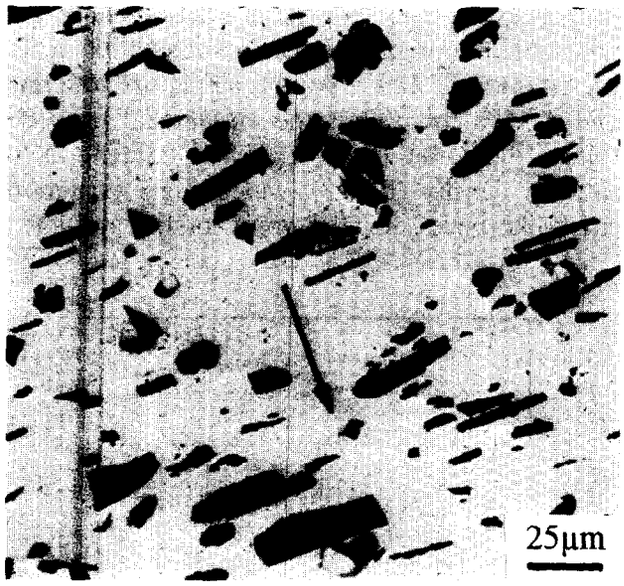

(a)

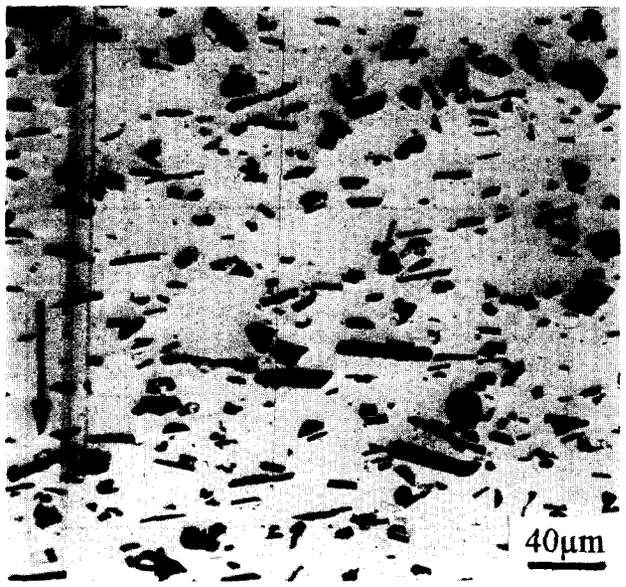

(b)

Fig. 8. SEM micrographs exemplifying the platelet orientation distribution in the BCEF planes (Fig. 6) over an area near to the porous mould face in bar samples, containing (a) 10 vol.% and (b) 20 vol.% SiC platelets. Arrows are perpendicular to the porous mould face.

The platelet alignment was attributed to the flow of water towards the porous mould surface, which is believed to tilt and rotate the platelets until they reach the interface of consolidation. However, the orientation distribution of platelets, although good, was not ideal as evident from the frequency–angle plots in Figs 6(a) and (b) and the corresponding micrographs (Figs 8(a) and (b)) which show some platelets in tilted positions with their basal planes at arbitrary angles to the slip-casting plane. The misorientation of platelets may be associated with variations in their geometry; as shown in Fig. 9, some of the as-received platelets have a low aspect ratio and some are very small and irregularly shaped, resembling particulate. It was concluded that the orientation distribution of platelets is most likely to be improved by control of the SiC_p reinforcement, particularly the aspect ratio which should be large (>10), than by further optimisation of the processing conditions.

Figure 10 shows the frequency versus angle plot, obtained from averaging the data from a number of areas across the complete cross-section (ABFG in Fig. 6) of a composite bar containing 20 vol.% SiC_p. The cross-sectional orientation profile of platelets is complicated with the presence of small peaks at a tilt angle of ~25° to the slip-casting plane, superimposed on the main preferred orientation peaks. The small peaks were

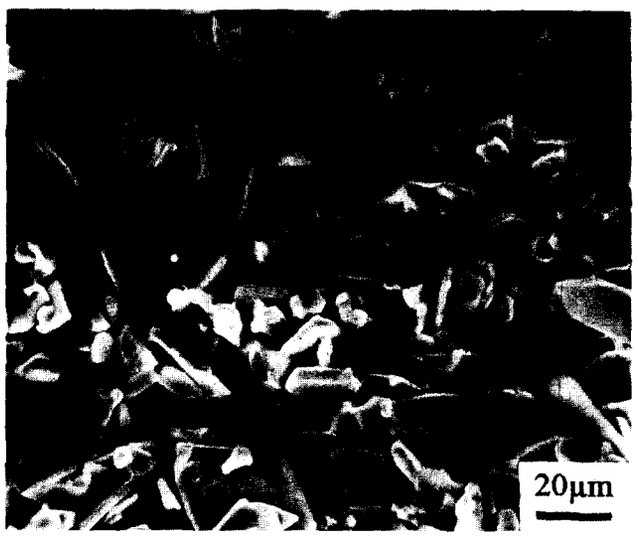

Fig. 9. SEM micrograph of as-received SiC platelets used in the production of composites.

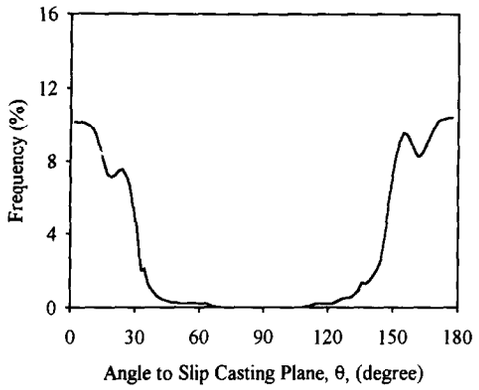

Fig. 10. The orientation distribution of SiC platelets in relation to the slip casting plane (the mould surface) observed in the ABFG planes (the cross-section in Fig. 6) of bar samples with 10 vol.% SiC platelet content.

associated with a V-shaped orientation distribution band of the platelets in the central regions of the cross-section (0·5 mm in thickness) between the porous faces of the mould (Fig. 11), whereas the rest of the cross-section has the same preferred orientation of platelets as that observed near to the porous face of the mould in section BCEF (Figs 7(b) and 8(b)).

It is known[27,28] that the capillary force of the mould, which forms the suction pressure to remove water from the slurry, becomes less effective with increasing thickness of the consolidated layer. This results in a highly reduced rate of water flow due to the pressure drop across the consolidated layer. Therefore, the central region of the cast between the faces of the mould is consolidated at a gradually reducing rate and the water flow rate is not high enough to induce a strong preferred orientation of platelets; this is partially because the SiC platelets increase the flow path of the water, as observed previously in slip casting whisker-reinforced ceramics.[10,29] Thus, the platelets are tilted under gravitational forces away from the preferred orientation, leaving them in a V-shaped configuration in central regions of the cast.

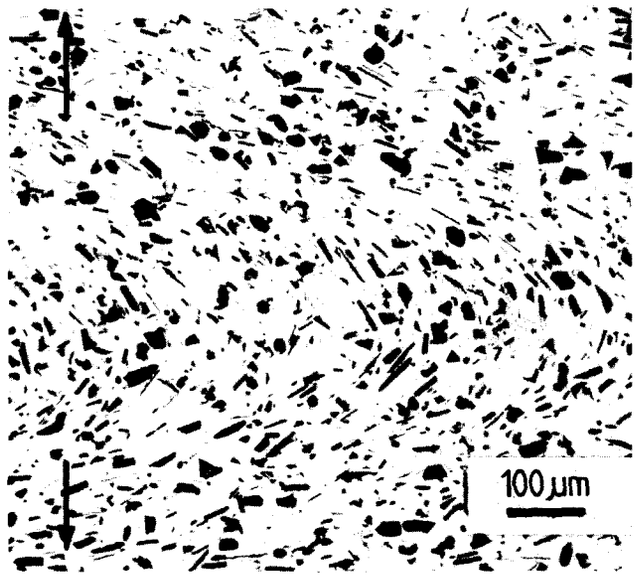

Fig. 11. SEM micrograph revealing V shaped orientation distribution of SiC platelets at the central regions of the cross-section (the ABFG plane in Fig. 6) of a composite bar, containing 20 vol.% SiC platelets. Arrows are perpendicular to the porous mould faces.

3.4 Influence of platelet content on mechanical properties

During strength and toughness testing, all composites exhibited a linear increase in stress with deflection; there was no evidence of non-linearity prior to catastrophic failure. The graphs of flexural strength and fracture toughness as a function of platelet content (Fig. 12 (a)) show that both these properties degrade with the platelet content. At 20 vol.% SiC_p content, the composite exhibits a flexure strength of 440 MPa and a fracture toughness of 6·4 MPa $m^{1/2}$. Thus the mechanical properties follow the same trend with SiC content as the sintered density (Fig. 3), which suggests that the crack-like pores, formed preferentially at some of

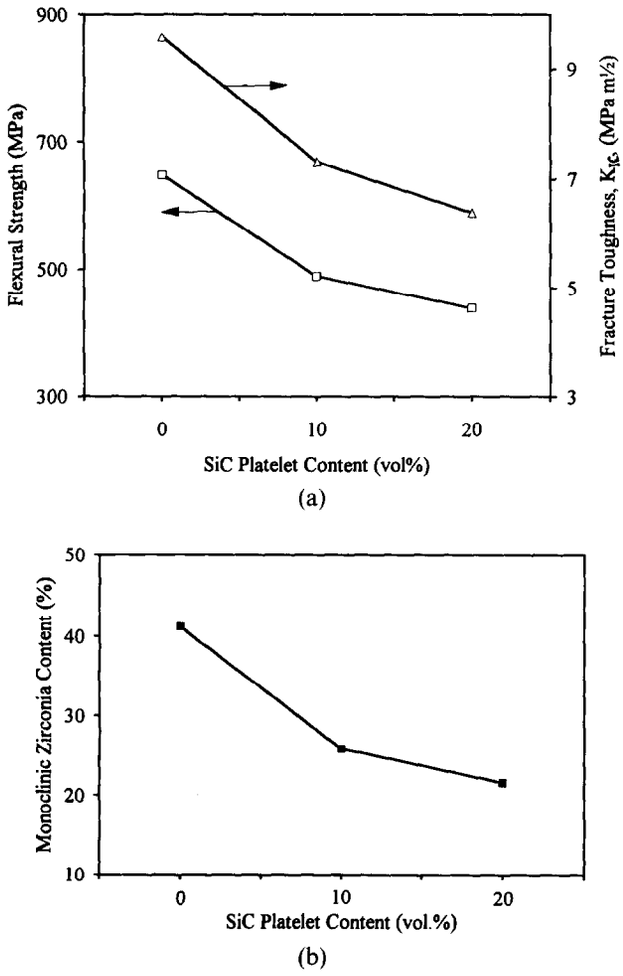

Fig. 12. (a) Flexural strength and fracture toughness of SiC_p-3Y-TZP composites as a function of volume fraction of SiC platelets and (b) the monoclinic zirconia content, determined by X-ray diffractometry at the fracture surfaces of SENB specimens, as a function of SiC platelet content.

the platelet–matrix interfaces, act as Griffith flaws on testing.

The reduced fracture toughness also suggests that the transformation-toughening mechanism in the matrix is hindered as the developing transformation zone at a crack tip is hampered by the incorporation of SiC platelets. Evidence for this type of behaviour was obtained from the determination of the monoclinic ZrO_2 content at fracture surfaces of SENB samples by X-ray diffractometry. The results plotted in Fig. 12 (b) show that the m-ZrO_2 content at fracture surfaces reduces with SiC platelet content. The decreasing fraction of transformed phase with increasing platelet content was attributed to a reduction in the transformation zone size due to platelets decreasing the stress intensity at a crack tip. Hence, the reduction in transformation toughening efficiency, together with the crack-like pores acting as flaws, lowers the strength and toughness with increasing platelet content. However, as the transformation toughening mechanism is unlikely to be significant in the monolithic material as the test temperature is raised, it is expected that the composite will exhibit relatively better, and perhaps even superior, toughness at elevated temperatures.

These explanations for the reduction in toughness with increasing SiC content requires strong interfacial bonding between the platelets and the matrix.[30] SEM observations of fracture surfaces of platelet containing specimens revealed that most of the platelets on the fracture plane had ruptured (Fig. 13 (a)), indicating that except where crack-like pores were present, the interfacial bonding was strong. As exemplified in Fig. 13 (b), the change of the crack plane from one platelet to another at the fracture surface suggests that there is some contribution of the crack deflection mechanism to toughening. Other toughening mechanisms, such as debonding and pull-out of platelets and crack bridging,[3–5] were not commonly observed due to strong interfacial bonding. Initial TEM studies of the platelet–matrix interfaces indicate the presence of amorphous films connected to sizeable pockets of glass. This will be reported in a future publication.

If the platelets are to contribute more effectively to the toughness of the composite, it is essential to eliminate porosity by applying an external pressure on sintering and to reduce the interfacial bond strength by additions of appropriate interfacial segregating species to the matrix, such as P, Si and Ti.

(a)

(b)

Fig. 13. Fracture surface of 3Y-TZP containing 20 vol.% SiC platelets, showing (a) the platelets ruptured on the fracture plane and (b) the crack deflection at platelets as indicated by arrows.

4 Conclusions

(1) Stable slurries of silicon carbide platelets (SiC_p) and yttria-stabilised tetragonal zirconia with good slip-casting properties have been produced with up to 75 wt% solid loading. Slurry processing at pH 3 by means of planetary milling, high-power ultrasonic dispersion and vacuum degassing resulted in a homogeneously dispersed composite slurry with minimal agglomeration.

(2) Slip casting of the composite slurries yielded relative green densities of 60%. A further increase in the green density of about 2% was achieved by cold isostatic pressing. Pressureless sintering at 1500°C for 3 h resulted in relative densities which fell with SiC_p content but were above 96%.

(3) There was a strong preferred orientation of the platelets with their basal planes parallel to the slip-casting plane, i.e. parallel to the porous mould faces, through the section of

the 48 mm × 12 mm × 10 mm bars. Overall misorientation of the platelets was attributed to variations in platelet geometry; the platelets with low aspect ratio and small size cannot be aligned to the preferred orientation by the force of water flow in the slurry. The misorientation of platelets in central regions of the cast was accounted for by the reduction in suction pressure across the consolidated cake and the gravitational forces tilting the platelets. The preferred orientation of platelets could be further enhanced by using SiC platelets with a larger aspect ratio.

(4) The room-temperature strength and toughness were found to reduce with platelet content. At 20 vol.% SiC_p content, the composite exhibited a flexure strength of 440 MPa and a fracture toughness of 6·4 MPa $m^{1/2}$. Analysis of fractography results indicated that crack deflection process may contribute to fracture toughness, but the crack-like voids, formed preferentially at the platelets, had an adversely predominant effect on both strength and toughness. The transformation toughening reduced with increasing platelet content and the toughening by debonding and pull-out of platelets could not occur due to strong interfacial bonding.

Acknowledgement

The authors gratefully acknowledge the funding provided by SERC award, grant number GR-F81729, and the supply of silicon carbide platelets by Third Millennium Technologies Inc., USA.

References

1. Lange, F. F., The interaction of a crack front with a second-phase dispersion. *Phil. Mag.*, **22**(179) (1970) 983–92.
2. Faber, K. T. & Evans, A. G., Crack deflection process. I. Theory. *Acta Metall.*, **31**(4) (1983) 565–76.
3. Marshall, D. B., Cox, B. N. & Evans, A. G., Mechanics of matrix cracking in brittle-matrix composites. *Acta Metall.*, **33**(11) (1985) 2013–21.
4. Homeny, J., Vaughn, W. L. & Ferber, M. K., Processing and mechanical properties of SiC-whisker–Al_2O_3-matrix composites. *Am. Ceram. Soc. Bull.*, **65**(2) (1986) 333–8.
5. Becher, P. F., Hsueh, C. H., Angelini, P. & Tiegs, T. N., Toughening behaviour in whisker-reinforced ceramic matrix composites. *J. Am. Ceram. Soc.*, **71**(12) (1988) 1050–61.
6. Claussen, N., Weisskopf, K. L. & Ruhle, M., Tetragonal zirconia polycrystals reinforced with SiC whiskers. *J. Am. Ceram. Soc.*, **69**(3) (1986) 288–92.
7. Birchall, J. D., Stanley, D. R., Mockford, M. J., Pigott, G. H. & Pinto, P. J., Toxicity of silicon carbide whiskers. *J. Mater. Sci Lett.*, **7** (1988) 350–52.
8. Sacks, M. D., Lee, H. W. & Rojas, O. E., Suspension processing of Al_2O_3/SiC whisker composites. *J. Am. Ceram. Soc.*, **71**(5) (1988) 370–9.
9. Lee, H. W. & Sacks, M. D., Pressureless sintering of SiC-whisker-reinforced Al_2O_3 composites: I. Effect of matrix powder surface area. *J. Am. Ceram Soc.*, **73**(7) (1990) 1884–93.
10. Hoffmann, M. J., Nagel, A., Greil, P. & Petzow, G., Slip casting of SiC-whisker-reinforced Si_3N_4. *J. Am. Ceram. Soc.*, **72**(5) (1989) 765–9.
11. Becher, P. F., Microstructural design of toughened ceramics. *J. Am. Ceram. Soc.*, **74**(2) (1991) 255–69.
12. Nischik, C., Seibold, M. M., Travitzky, N. A. & Claussen, N., Effect of processing on mechanical properties of platelet-reinforced mullite composites. *J. Am. Ceram. Soc.*, **74**(10) (1991) 2464–8.
13. Baril, D. & Jain, M. K., Evaluation of SiC platelets as a reinforcement for oxide matrix composites. *Ceram. Eng. Sci. Proc.*, **12** (1991) 1175–92.
14. Stewards, N. I., The influence of particle size distribution on the sintering of ceramic powder compacts. PhD Thesis, Imperial College of Science and Technology, London, 1989.
15. Brown, W. F. & Srawley, J. E., Plain strain crack toughness testing of high strength metallic materials. ASTM Special Technical Publication, No.410, American Society for Testing and Materials, 1966.
16. Toraya, H., Yoshimura, M. & Somiya, S., Calibration curve for quantitative analysis of the monoclinic–tetragonal ZrO_2 system by X-ray diffraction. *J. Am. Ceram. Soc.*, **67** (1984) C119–121.
17. Melluish, I. & Konsztowicz, K. J., The effects of surface treatment of SiC whiskers on rheological properties of their aqueous suspensions. In *Proc. Int. Symp. Advances in Processing of Ceramic and Metal Matrix Composites*, ed. S. Mostaghaci. Pergamon Press, 1989, pp. 15–26.
18. Adair, J. H., Mutsuddy, B. C. & Drauglis, E. J., Stabilisation of silicon carbide whisker suspensions: I. Influence of surface oxidation in aqueous suspensions. *Adv. Ceram. Mater.*, **3**(3) (1988) 231–4.
19. Nikumbh, A. K., Schmidt, H., Martin, K. & Porz, F., Slip casting of partially stabilised zirconia. *J. Mater. Sci.*, **26** (1991) 3649–56.
20. Konsztowicz, K. J., Ultrasonic homogenization of dense colloidal suspensions of SiC_w/Al_2O_3 composites. *Ceram. Eng. Sci. Proc.*, **11**(7–8) (1990) 695–708.
21. Heussner, K. H. & Claussen, N., Yttria- and ceria-stabilised tetragonal zirconia polycrystals (Y-TZP, Ce-TZP) reinforced with Al_2O_3 platelets. *J. Eur. Ceram. Soc.*, **5** (1989) 193–200.
22. Sudre, O. & Lange, F. F., Effect of inclusions on densification: I. Microstructural development in an Al_2O_3 matrix containing a high volume fraction of ZrO_2 inclusions. *J. Am. Ceram. Soc.*, **75**(3) (1992) 519–24.
23. Sudre, O., Bao, G., Fan, B., Lange, F. F. & Evans, A. G., Effect of inclusions on densification: II. Numerical model. *J. Am. Ceram. Soc.*, **75**(3) (1992) 525–31.
24. Lange, F. F., Constrained network model for predicting densification behaviour of composite powders. *J. Mater. Res.*, **2**(1) (1987) 59–65.
25. Tuan, W. H. & Brook, R. J., Sintering of heterogeneous ceramic compacts, Part 2. ZrO_2–Al_2O_3. *J Mater. Sci.*, **24** (1989) 1953–8.

26. De Jonghe, L. C., Rahaman, M. N. & Hsueh, C. H., Transient stresses in bimodal compacts during sintering. *Acta Metall.*, **34**(7) (1986) 1467–71.
27. Hampton, J. H. D., Savage, S. B & Drew, R. A. L., Experimental analysis and modelling of slip casting. *J. Am. Ceram. Soc.*, **71**(12) (1988) 1040–5.
28. Tiller, F. M. & Tsai, C. D., Theory of filtration of ceramics: I. Slip casting. *J. Am. Ceram. Soc.*, **69**(12) (1986) 882–7.
29. Chouh, Y. S. & Green, D. J., Silicon carbide platelet/alumina composites: I. Effect of forming technique on platelet orientation. *J. Am. Ceram. Soc.*, **75**(12) (1992) 3346–52.
30. Poorteman, M., Descamps, P., Cambier, F., Leriche, A. & Thierry, B., Hot isostatic pressing of SiC-platelets Y-TZP composites. *J. Eur. Ceram. Soc.*, **12**(2) (1993) 103–9.